Earth Systems and Environment
https://doi.org/10.1007/s41748-024-00526-6

ORIGINAL ARTICLE

Decadal Variability of Dry Days in Central Chile

Daniela Latoja[1] · Mario Lillo-Saavedra[2] · Consuelo Gonzalo-Martin[3] · Alex Godoy-Faúndez[1] · Marcelo Somos-Valenzuela[4] · Diego Rivera[1]

Received: 27 July 2024 / Revised: 11 November 2024 / Accepted: 15 November 2024

Abstract
Dry days are crucial in precipitation variability and water scarcity, particularly in Mediterranean regions facing increasing aridity. Despite their importance, most research focuses on precipitation amounts and temporal dynamics. This study addresses this gap by analyzing dry days' temporal and spatial variability in central Chile (32–40 S), a region experiencing prolonged drought. We examined dry day patterns from 1960 to 2021 using high-resolution gridded precipitation data, defining dry days with five precipitation thresholds (0.10, 1, 2.5, 5, and 10 mm/day). Principal component and trend analyses were employed to characterize spatial and temporal variability. Results reveal a spatial pattern of dry days closely following precipitation patterns, with more dry days in northern and coastal areas. The first principal component explains 70–80% of the variance, and clustering methods allowed the definition of five homogeneous regions with distinct monthly dry-day characteristics. Long-term trends show a significant increase in annual dry days south of 38°S, while trends are weaker and non-significant further north. Notably, trend direction is highly sensitive to the analysis period, with some regions showing opposing trends before and after 1982. The 2010–2019 megadrought is detectable in decadal anomalies. We found links between dry day anomalies and large-scale climate patterns, suggesting modulation by changes in subtropical and extratropical atmospheric circulation. This comprehensive characterization of dry day climatology and variability provides crucial insights for water resource management and climate change adaptation in central Chile and similar Mediterranean regions worldwide. Our findings highlight the importance of considering dry day frequency in drought assessment and water planning, contributing to a more nuanced understanding of precipitation patterns in Mediterranean climates.

Keywords Water management · Temporal trends · Climate variability

1 Introduction

Annual precipitation totals are associated with a sequence of dry and wet days, frequently defined as days with lower or higher precipitation than a specific threshold. The pace of this sequence influences the dynamics of water availability and water management. The change in the number of dry days tends to dominate annual changes in precipitation in many places of the world (Polade et al. 2014a; Tabari and Willems 2018). Chen and Dai (2018) suggest that frequency changes are more important than intensity changes in determining accumulated precipitation variations. Moreover, in extratropical areas and Central and South America, the number of dry days within the year would increase up to 30 more dry days by the end of this century (Ma et al. 2015; Rivera et al. 2013; Polade et al. 2014a; Giorgi et al. 2019; IPCC 2021).

✉ Diego Rivera
diegorivera@udd.cl

[1] Facultad de Ingeniería, Universidad del Desarrollo, Avenida Plaza 600, Santiago, Chile

[2] Facultad de Ingeniería Agrícola, Universidad de Concepción, Vicente Méndez 595, Chillán, Chile

[3] Computer School, Universidad Politécnica de Madrid, Boadilla del Monte 28660, Madrid, Spain

[4] Facultad de Ciencias Agropecuarias y Medioambiente, Universidad de La Frontera, Avenida Francisco Salazar 01145, Temuco, Chile

Published online: 21 November 2024

Dry days are relevant for water management (IPCC 2021). More frequent dry days would affect agricultural production and determine policy options due to expected shifts in precipitation (Hettiarachchi et al. 2022) as annual precipitation means are related to changes in dry days frequency and daily precipitation on wet days (Pierce et al. 2013). Thus, characterizing changes and drivers in the frequency of dry and wet days can mitigate crop damage and losses through more efficient water management practices (Wetterhall et al. 2015). Indeed, projected long-term changes in daily precipitation, such as the number of dry days, have been linked to contribution to an overall increase in precipitation variability and, consequently, affecting the planning and management (Polade et al. 2014b), as precipitation deficit cascade to hydrological deficits and hydrological droughts depending on catchment wetness and seasonality of the regime (Van Loon and Laaha 2015; Apurv et al. 2017).

Central Chile (32°-40°S) has a Mediterranean-type climate -warm, dry summers and temperate-to-cold wet winters (Sarricolea et al. 2017). Winter precipitation accounts for 90–70% of annual amounts, from North to South (Pica-Téllez et al. 2020) (Fig. 1). Precipitation is stored in natural -snowpack and groundwater recharge- and artificial -dams and reservoirs- systems where water availability for people, ecosystems, and productivity largely depends upon winter precipitation (Valdés-Pineda et al. 2016). South of 36°S, summer precipitation is higher and more significant to agriculture, which relies on spring precipitation, snowmelt, and summer rainfall to complement irrigation sourced from surface water. Expected and already recorded less summer rainfall or more prolonged periods with no rain would require supplement irrigation or increased groundwater use. A drier summer south of 38°S would affect agricultural production as the current infrastructure could not suffice for the new water regime (Barria et al. 2019). Moreover, observed changes in precipitation indices could manifest a new hydrological regime (Fernández et al. 2018) with a decrease in water yield (Martínez-Retureta et al. 2021; Boisier et al. 2018b).

In Central Chile, annual precipitation shows a negative trend of 15 to 45% of annual amounts (2010–2018) (Boisier et al. 2018b, 2024; Boisier 2023). Winter deficits are related to fewer frontal systems hitting Chile (Montecinos et al. 2011). Since 2010, fewer frontal systems have reached the country, even though El Nino Southern Oscillation (ENSO) neutral conditions have prevailed. Also, there is an increase in rainfall concentration (Sarricolea et al. 2019; Sanguüesa et al., 2018), along with decreasing stream flows, impacting water availability (Barria et al. 2019). Temperatures show positive trends from 1979 to 2015 but differ among seasons (Burger et al. 2018). The negative trends in seasonal precipitation and associated temperatures along continental Chile could be explained by the combination of the Hadley Cell expansion and the circulation induced by the Sea Surface Temperature Southern Blob - a region in subtropical southwest Pacific showing a marked surface warming over the last decade (Lagos-Zúñiga et al., 2024; Garreaud et al. 2021). Also, Boisier et al. (2018b) indicates that Antarctic stratospheric ozone depletion has played a major role in the decline of summer rainfall.

Current conditions in Central Chile show significant precipitation and hydrological deficits, leading to gaps between water demand and supply. This situation underscores the urgent need for enhanced water management strategies to accommodate the increasing water demand. Several studies have examined the variability in accumulated precipitation, yet the changes in the frequency and distribution of dry days throughout the year still need to be studied. The article's goal is to describe the temporal and spatial changes in dry days at monthly, yearly, and decadal scales, examining how these changes affect precipitation totals and interannual variability. Initially, we analyze the temporal and spatial patterns of dry days. Subsequently, we investigate dry days' modes of variability and temporal trends to determine the significance of changes across different time scales and their relationship with climatological fields. The last section also discusses the implications of our findings on the preparedness of communities and policymakers.

2 Data and Methods

2.1 Study Region

We focus our study on Central Chile (32 °S to 40 °S) since most of the Gross Domestic Product related to agriculture comes from this region. Agriculture uses 85% of available freshwater (Ministerio del Medio Ambiente, 2020).

More than 90% of the study area falls into the Csb Koppen-Geiger climatic classification (Sarricolea et al. 2017). The Csb classification stands for a temperate climate (C) with a summer dry season (s) and a warm thermal regime (b). The daily mean temperature during the summer is 20 °C and 12 °C during winter. The precipitation of the driest month in summer is less than 40 mm. The rest of the area has cold climates in the mountains (Sarricolea et al. 2017). The Andes induce an orographic effect, resulting in precipitation amounts at the slopes that double the valley's precipitation (Boisier et al. 2018b).

Central Chile experiences strong seasonal (Montecinos et al. 2000; Garreaud et al. 2016), interannual (Garreaud et al. 2017a; Montecinos et al. 2000, 2011), and decadal climate variability (Garreaud et al. 2009; Valdés-Pineda et al. 2018; Núñez et al. 2013). Winter precipitation events occur

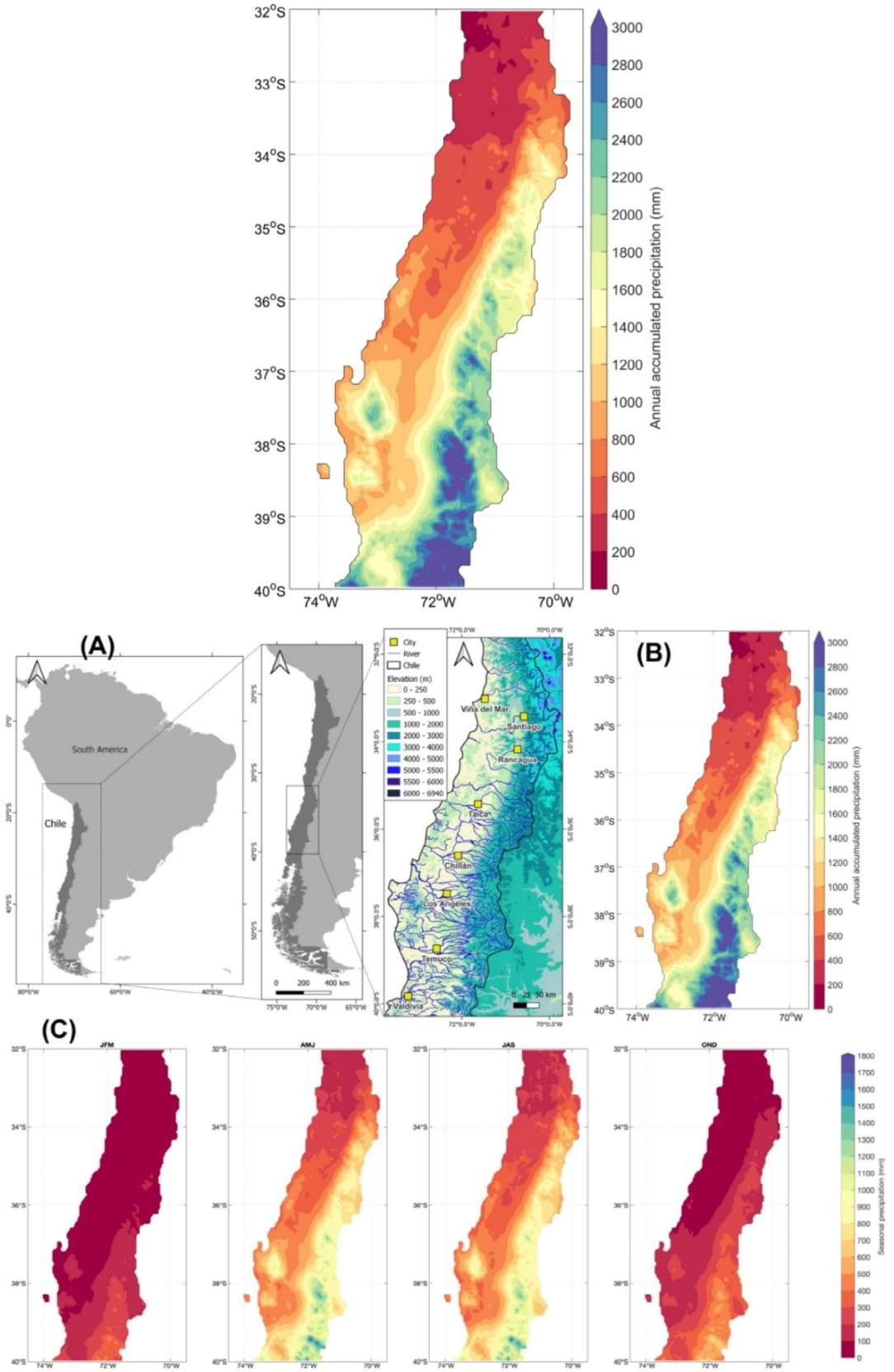

Fig. 1 (**A**) Location, topography, and river network of the study area (**B**) Annual mean (1960–2021) accumulated precipitation over central Chile (**C**) Seasonal means (1960–2021) of precipitation

as midlatitude frontal systems pass through the west coast of southern South America (Rutllant and Fuenzalida 1991; Montecinos and Aceituno 2003; Garreaud 2009; Garreaud et al. 2009; Catto et al. 2012), where the presence of The Andes induces an orographic enhancement of precipitation, causing a longitudinal gradient of rainfall (Garreaud 2009; Viale and Garreaud 2015). The seasonal variability of the South Pacific High, its latitudinal/longitudinal displacements and intensity changes, exerts control over seasonal precipitation (Barrett and Hameed 2017). Less winter precipitation is related to fewer frontal systems hitting the country (Montecinos et al. 2011). The Southern Hemisphere's storm track exhibits seasonal variability, implying that cyclonic activity extends up to 30°S during austral winter (Hoskins and Hodges 2005) and remains mostly south of 40°S during summer, producing a marked latitudinal gradient of accumulated precipitation (Fig. 1).

2.2 Data Sources

We used a high resolution (0.05° × 0.05°, 5×5 km) daily precipitation gridded product developed by the Center of Climate and Resilience Research (CR2), which encompasses all continental Chile and spans the period 1960–2021. This dataset, henceforth.

CR2MET, applies statistical downscaling methods to meteorological station data and reanalysis data (ERA5), also considering topography and its effect on precipitation (Boisier et al. 2018a; Boisier 2023). We chose this product over raw meteorological station data because, in such case, a profound selection and homogenization work must be done, and we consider that the development of CR2MET has already solved this problem. The data has been extensively used in climate studies in Chile as it relies on official records from government agencies and passed strict quality control (e.g. Zambrano et al. 2017; Zambrano-Bigiarini et al. 2017).

2.3 Methods

We defined dry days as daily precipitation under a given threshold. We explored five thresholds, 0.1, 1, 2.5, 5, and 10 mm (Cindric et al. 2010; Zolina et al. 2013; Polade et al. 2014a; Marinovic et al. 2021; Bartolini et al. 2022). We generated binary time series where 1 corresponds to daily precipitation less than the threshold and 0 otherwise.

The effect of threshold magnitude on precipitation statistics is an open question since different factors, such as local climatic features, the aim of the study, and source data, among others, could influence threshold selection. Thresholding could be classified into constant values for the whole spatial domain (e.g. Zolina et al. 2013; Wang et al. 2022; Motamedi et al. 2023) and variable values for each subdomain -station or pixel- depending on percentiles (Ratan and Venugopal 2013). However, 0.1 mm and 1 mm are the most utilized thresholds (e.g. Bartolini et al. 2022). Moreover, Polade et al. (2014a) suggests using a 1 mm/day threshold for consistency between models and observations. Dry-day thresholds should account for different types of climate, if present, in the study area using, for instance, percentiles (e.g. Motamedi et al. 2023). In this case, we chose a constant threshold but five different levels as the spatial domain displays a similar precipitation pattern and forcing.

The workflow for analyzing dry days in central Chile consists of two main branches: data preprocessing and analysis of the CR2MET daily precipitation dataset (19602021) and climate data analysis using ERA5 reanalysis and HadISST sea surface temperature data (Fig. 2). The ERA5 data set is a global atmospheric reanalysis (hourly estimates) from 1940 to the present in a 31 km grid produced by the European Centre for Medium-Range Weather Forecasts (ECMWF) (Hersbach et al. 2020). The data preprocessing branch defines dry day thresholds (0.1, 1, 2.5, 5, and 10 mm/day), and binary time series are generated to identify dry days. These binary time series are then aggregated into monthly and annual scales. The aggregated data is passed to the data

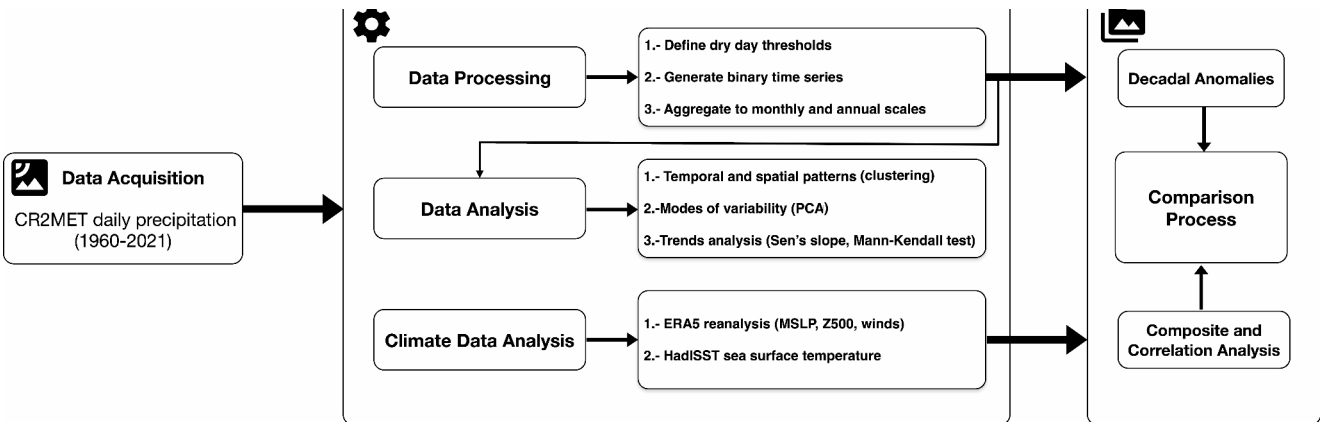

Fig. 2 Workflow for dry days analysis

analysis branch, where temporal and spatial patterns, modes of variability (using Principal Component Analysis, PCA, and clustering), trends analysis (using Sen slope and Mann-Kendall test), and decadal anomalies are investigated. For the climate analysis, we used the following variables from ERA5 reanalysis: precipitation, Mean Sea Level Pressure (MSLP), Geopotential Height at 500 hPa (Z500), and horizontal wind at 250, 500, and 850 hPa (V250, V500, and V850, respectively). For Sea Surface Temperature (SST), we used the Hadley Centre Global Sea Ice and Sea Surface Temperature (HadISST) data, which is a combination of monthly globally complete fields of SST and sea ice concentration for 1871-present (Rayner et al. 2003) to perform composite and correlation analyses. This workflow allows for a comprehensive understanding of the dry day variability in central Chile and its relationship with large-scale climate patterns.

We aggregate the dry days per month and year using the binary time series and calendar dates. Since, in this case, we are not considering the consecutiveness of dry days, we can calculate statistics over these time ranges, notwithstanding that they do not depict the time frames of natural variability. Following calendar dates, we counted the dry days for each 744 months (62 years) in the time series per pixel. Then, we calculated the mean for each one of the 62 values for January, and so on. We divided the monthly (yearly) values by their standard deviation for standardization. Thus, we obtained a pixel-wise time series of (1) the number of dry days per month, (2) the percentage of dry days per month, and (3) the number of dry days per year. Standardization is advantageous because equal weight and absolute-value bias are avoided, such as the effect of precipitation magnitude and watershed contributing areas are equalized (Wilks 2005).

Identifying spatial variability patterns involves determining geographical locations where certain environmental variables display common features (Rubio-Alvarez and McPhee 2010). Hierarchical clustering groups data points into clusters based on their similarity, but it is sensitive to noise outliers, and the choice of variables can affect the hierarchy. Here, we applied hierarchical clustering using Ward's linkage method to converge pixel-wise time series into fewer signals and homogeneous areas, facilitating the description of the behavior of the different regions of the study zone. Grouping features are annual median values and dispersion (interquartile range). However, here, we assume it might be possible to define a "homogeneous region" from pixel data related through clustering. So, it must be pointed out that the aim of applying this clustering is merely operational and only considers the statistical aspects of dry days. A robust regionalization of dry days is beyond the scope of this study.

We performed a PCA analysis pixel-wise at monthly and annual scales to examine joint temporal variability from a different view. PCA in S-mode, also known as empirical orthogonal functions (EOF), is a widely utilized technique in multivariate statistical analysis that reduces the number of variables of a data set by creating new ones from linear combinations of the original ones (Wilks 2011). By doing this, most of the variability is often concentrated in a few main variables (Jolliffe 2005), so the subsequent analysis is facilitated. We retained principal components considering the percentage of explained variance. However, it should also be highlighted that these newly generated variables and their respective representative spatial patterns do not necessarily depict a physical feature of the phenomenon. Therefore, their interpretation must be cautious (Dommenget and Latif 2002).

We examined temporal variability by calculating linear trends at every pixel by the Sen-Theil estimator, which is more robust than the trend estimation through the least squares fit (Wilks 2011; Rubio-Alvarez and McPhee 2010), and a modified Mann-Kendall test, suitable for autocorrelated data (Hamed and Rao 1998), to verify statistical significance at 95% confidence level at each pixel. We analyzed average decadal anomalies of monthly and annual dry days to inspect temporal variability at decadal time scales. Significance was tested using a two-tailed t-test, also at a 95% confidence level. Mann-Kendall Trend Test is a non-parametric test that detects increasing or decreasing monotonic trends. The null hypothesis is that there's no trend for the times series' timespan, while the alternative hypothesis suggests a trend exists.

To explore the climatological conditions related to the occurrence and variability of dry days, we used composites (mean condition for a given period and location). The SLP fields allow the identification of the high and low-pressure centers, as the Pacific Anticyclone; the zonal wind fields allow the analysis of the westerly wind belt, while the SST field is the main predictor for ENSO phases and related changes in precipitation (Arias et al. 2021; Aceituno et al. 2021; Garreaud et al. 2009). We also analyzed atmospheric fields from ERA5 reanalysis data (Hersbach, 2019) in the South Pacific area over the study period. We examined monthly mean MSLP, Z500, and horizontal wind fields V250, V500, and V850, respectively). Additionally, we analyzed sea surface temperature (SST) data from HadISST. Considering these variables, we applied a composite analysis using average decal anomalies and compared them with the decadal anomalies of dry days.

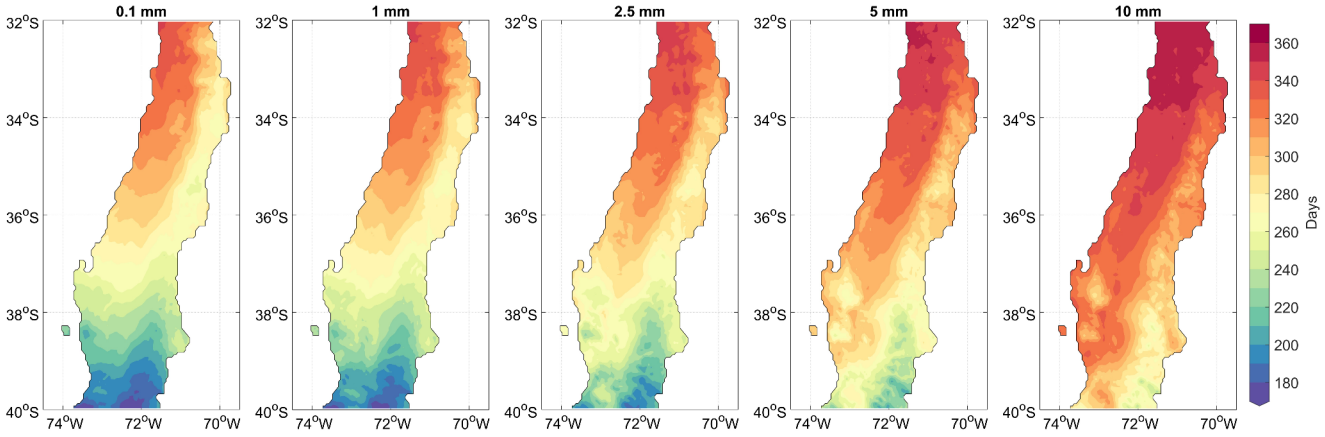

Fig. 3 Annual mean accumulated dry days from 1960 to 2021 using five different thresholds to define dry days

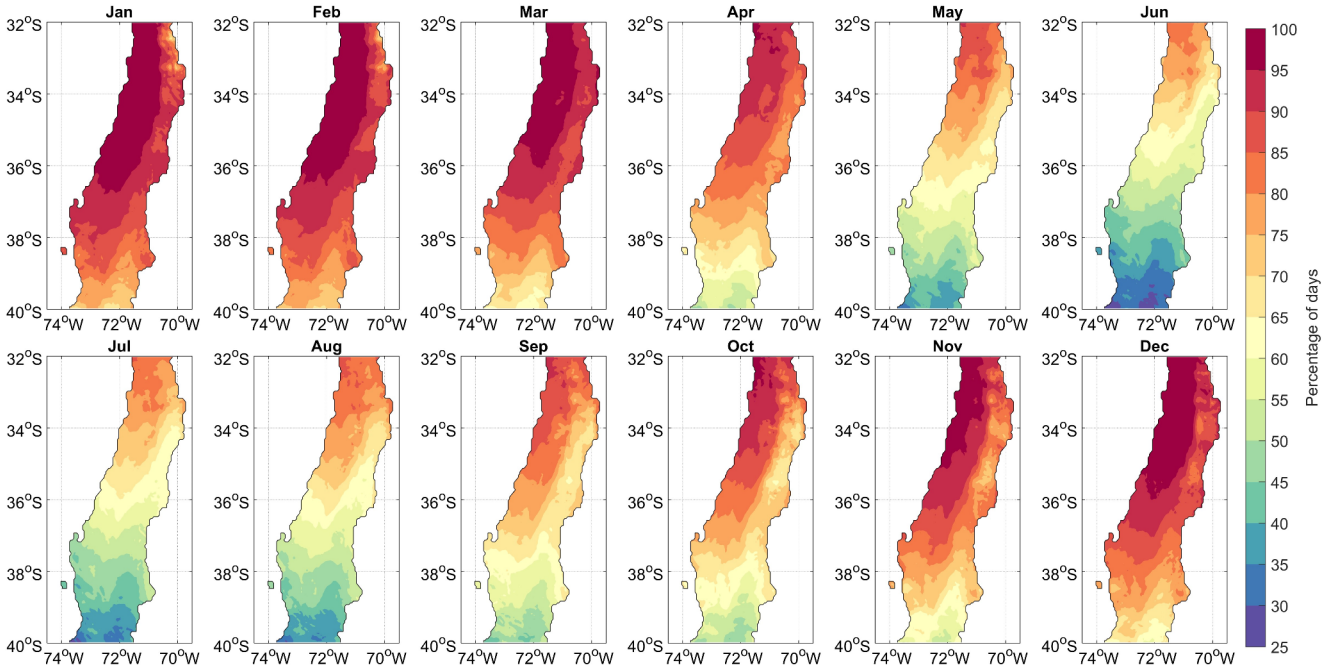

Fig. 4 Average monthly accumulated dry days, shown as a percentage for the number of days in the corresponding month, on the period 1960–2021 and using a threshold of 1 mm/day for the definition of dry days

3 Results

3.1 Spatial Patterns

For the period 1960–2021, mean values of dry days per year (Fig. 3) show a similar spatial distribution to precipitation annual means (Fig. 1) for all thresholds (0.1, 1.0, 2.5, 5.0, and 10 mm per day). The 0.1 and 1 mm thresholds yield similar results, as the CR2 data likely does not capture low precipitation events as precipitation frequency and intensity estimates are sensitive to the spatial and temporal resolution of input data (Chen and Dai 2018). From north (32°S) to south (40°S), dry days decrease as the total precipitation amounts increase. Also, coastal and valley areas have more dry days than mountain areas. However, the spatial distribution depends upon the threshold. The number of dry days in the southern sector shows a higher sensitivity to the different thresholds (comparing 0.1 to 10 mm). Dry days per year north of 36°S are more than 300 days for all thresholds, exceeding 360 days per year with less than 10 mm/ day.

For completeness' sake, we present the percentage of dry days per month for 1 mm of precipitation per day as a threshold (Fig. 4) since it is one of the most.

utilized thresholds in literature (Cindric et al. 2010; Zolina et al. 2013; Bartolini et al. 2022; Anagnostopoulou et al. 2003). In Fig. 4, seasonal rainfall variability can be

observed: wet days concentrate during winter months (JJA), and dry days dominate during summer, especially north of 36°S. More than two-thirds of dry days occur during six months (JFM, OND). The lowest dry days over the study zone for all thresholds occurs in June, while the highest occurs in January and February. A latitudinal gradient of monthly dry days can also be observed for all thresholds and is present throughout the year. Differences in winter north and south 38°S result from winter precipitation amounts.

3.2 Modes of Variability and Clustering

Figure 5 shows the first modes of variability from pixel-wise principal component analysis of annual accumulated dry days standardized anomalies. The first two Principal Components explain more than 80% of the variance. The spatial pattern for PC1 is similar for all thresholds, reflecting high joint variability as per correlation and explained variance high values (over 70% for all thresholds). However, the variability of the very northern (32–33°S) and southern sectors (39–40°S) is less represented by PC1, especially in the cases of lower thresholds. The north band is a transition to a semi-arid climate, and the south shows the influence of the coastal range (Cordillera de Nabuelbuta; Garreaud et al. 2016). The time series for PC1 are similar in all 5 cases, reflecting interannual variability. PC1 also shows long-term variability (Figure.

5), and we observe an inflection point around 1982 from negative to positive trends. PC2 (figure not shown) explains much less variance than PC1 (around 12%), and its time series suggests interannual and interdecal variability. The respective spatial field of PC2 indicates a dipole between the northern (32–34°S) and southern sectors (3840°S). Higher-order PCs are not discussed here since the explained variance is legible, and their spatial fields do not show clear patterns.

On the other hand, we grouped pixels through hierarchical clustering, considering statistics of dry days for all thresholds. We show clustering results using 0.1 mm (Fig. 6) since the resulting clusters display spatial noise. We limited the number of clusters to five to facilitate the analysis and avoid over-clustering pixels with similar climatological-statistical features (Cluster 1 is the northernmost one). Figure 6 displays the cluster average time series of standardized dry days per year and standardized annual precipitation. First, interannual variability is observable, and both time series follow opposite year-to-year directions, i.e., higher dry days anomalies imply lower precipitation anomalies. The coefficient of determination r^2 derived from Pearson's correlation between dry days and precipitation anomalies is significant for all clusters.

The highest r^2 values appear for 2.5 mm per day as the threshold, followed by 10 mm per day as the threshold. r^2 decreases southwards from Cluster 1.

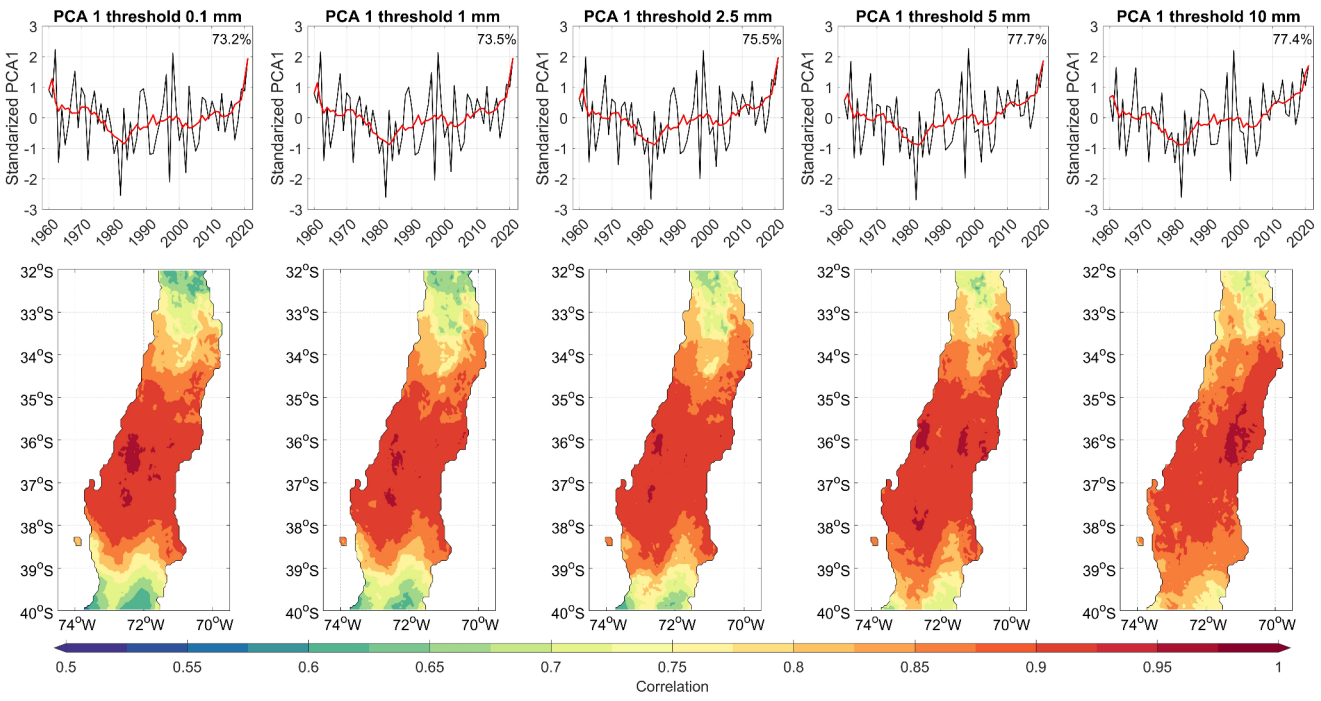

Fig. 5 Upper panel: First principal component of the annual dry days' field for each threshold and percentage of explained variance by the first mode of variability. The black line corresponds to the annual time series, and the red line corresponds to the smoothed series with a 10-year running mean. Lower panel: Correlation patterns between the first principal component and the original pixels' time series of dry days

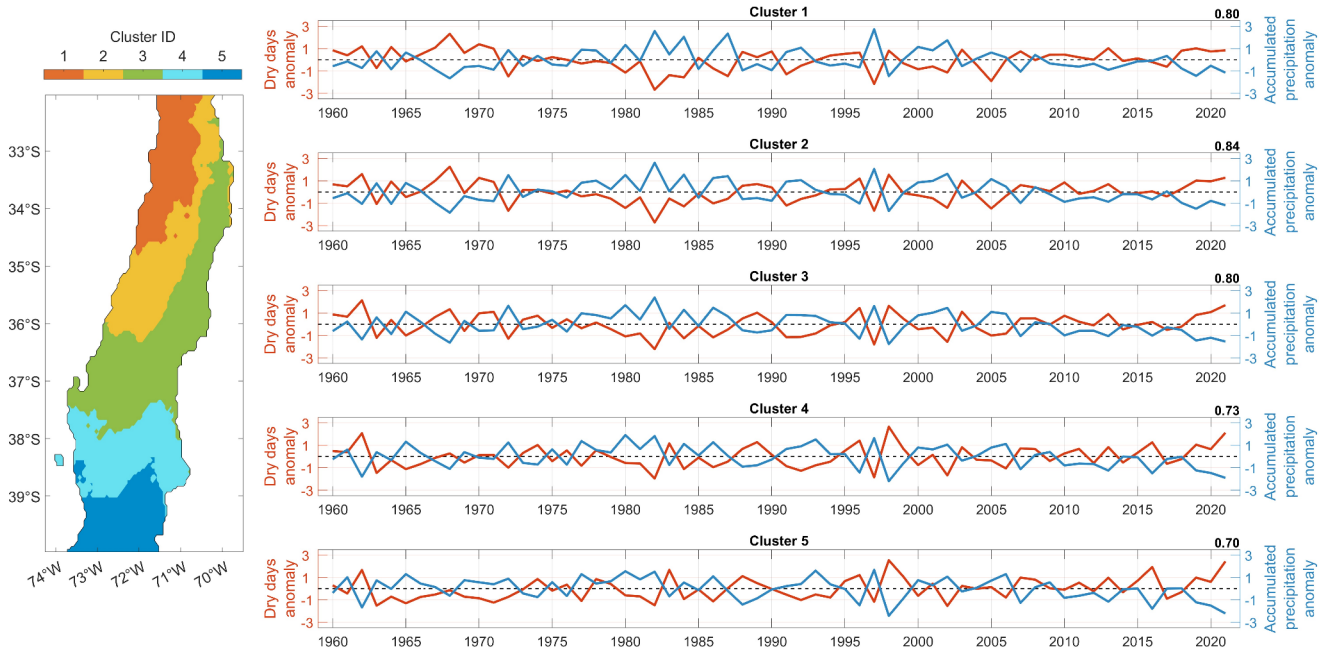

Fig. 6 Left panel: Spatial cluster using average and dispersion values of annual dry days using a 0.1 mm per day threshold. The numbering follows the average latitude of their corresponding pixels. Right panel: Time series of average (per cluster) standardized anomalies of annual accumulated dry days (red) and accumulated precipitation (blue) over the study period 1960–2021. The number on the top right corner of each graph corresponds to the coefficient of determination r^2 between the corresponding time series

Dry-day anomalies tend to peak simultaneously on all clusters, supporting a robust spatial coherence derived from the precipitation pattern. Among clusters (Figs. 5 and 6), the first mode of variability is highly representative of clusters 2, 3, and 4 in terms of magnitude and variability. Clusters 1 and 5 show similar variability to PC1, although magnitudes differ since these clusters are also represented (although to a lesser extent) by PC2.

Monthly precipitation and dry days anomalies strongly share variance. However, the strength of this relationship varies in space and time and also depends on the threshold used to define a dry day. For example, in summer months, when precipitation.

events are scarce, r^2 values could reach lower values than 10% in some areas. Therefore, one should be cautious in determining changes and variability of one variable from the behavior of the other, especially when short time scales, such as months, are considered. On longer time scales (season or year-round), r^2 values are more consistent and generally allow us to consider a more robust relationship between accumulated precipitation variations and dry days in central Chile.

3.3 Trends for non-overlapping Periods

Trends' signs in dry days anomalies (Fig. 6) are generally opposite for periods 1960–1982 and 1983–2021 (Table 1). A relative minimum of dry days appears in 1982 for clusters 1 to 4. Clusters 1 to 3 show significant trends of opposite signs before and after 1982 for dry days and accumulated precipitation, but trends on the entire period are usually non-significant. For clusters 4 and 5, trends of dry days before and after 1982 are not all significant, although there are significant and negative trends of accumulated precipitation in these two clusters (1960–2021). Significant trends of dry days for the entire period can only be observed in cluster 5 (positive trends).

Table 1 Sen's slope and Mann-Kendall test for average time series at each cluster

Cluster	1960–2021	1960–1980	1981–2021
Cluster 1	0.003	-0.028	0.033*
Cluster 2	0.007* 4	-0.049	0.034*
Cluster 3	0.011	-0.061 8	0.041*
Cluster 4	0.014	-0.026	0.043*
Cluster 5	0.019*	-0.012	0.034*

*Statistically significant at 95% confidence level

Moreover, limited areas show significant positive trends of dry days per year (Fig. 7, upper panel) for 1960–2021 (all thresholds), especially the southern sector, as previously mentioned. Over this latter area, particularly south of 38°S, trends are mainly statistically significant and higher in magnitude, indicating an increase of annual dry days up to 5–6 days per decade. North of 38°S, nonsignificant trends suggest 1 or 2 more dry days per decade. Trends per month (figure not shown) reveal considerable variability. March,

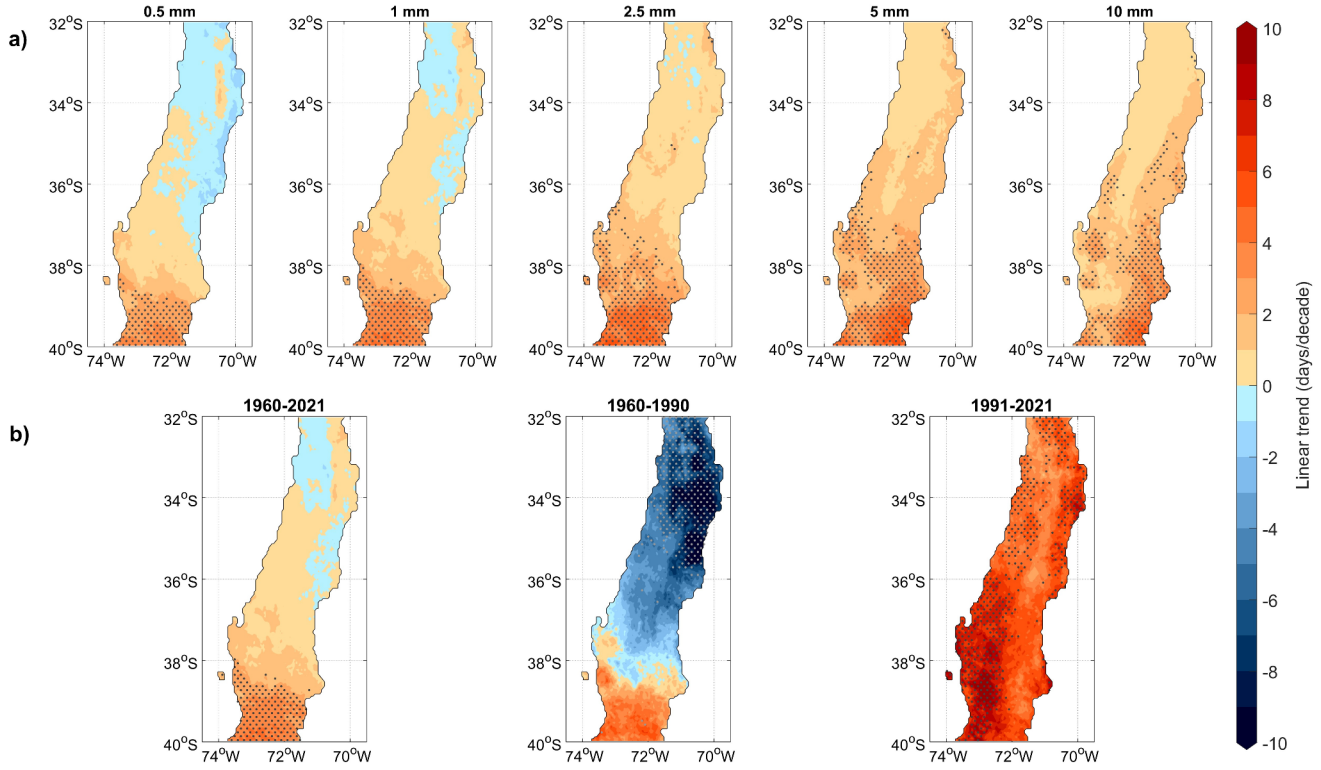

Fig. 7 (**a**) Linear trends of annual accumulated dry days from 1960–2021 for each threshold. (**b**) Linear trends of annual accumulated dry days on different periods considering a threshold of 1 mm for defining dry days. In both panels, stippled areas indicate statistical significance at 95%

June, October, and December exhibit small to no trends, regardless of the threshold, while others may exhibit both positive and negative trends. For instance, May's trends (0.1 and 1 mm per day thresholds) are decreasing north of 38°S and positive south of this latitude. For higher thresholds, negative trends disappear, and very positive trends reduce their spatial extent. In general, months with higher positive and significant trends south of 38°S are May, July, and September, so annual trends shown in Fig. 7 can be attributed to more significant changes occurring in these months.

To compare not overlapping periods, we show trends for 1960–2021, 1960–1990, and 1991–2021 of pixel-wise annual accumulated dry days for 1 mm/day threshold (Fig. 7, lower panel). We did not split in 1982 to compare trends on periods of similar length. Differences between these 3 cases are remarkable. During the first half, trends are primarily negative (wettening) north of 38°S, while south of 38°S trends are mainly positive and non-significant. From 1991 to 2021, trends were positive and statistically significant throughout the study zone, especially in valley and coastal areas. Thus, opposing trends north of 38°S for 1960–1990 and 1991–2021 yielded positive but relatively small long-term trends, depicting a high decadal variability.

Monthly trends vary considerably. During 1960–1991, several months (March, April, May, and September) exhibited negative trends over large areas and were primarily statistically significant. Positive trends mainly appeared in winter months and south of 36°S, with limited areas showing statistical significance. During 1991–2021, negative trends dominated from March to June for all thresholds, although magnitude and significant regions also tend to decrease for higher thresholds. April's positive and significant trends are mainly present over almost the entire study zone, but opposite trends before and after 1990, similar to May. Positive trends dominate in the two subperiods for June, but the spatial pattern differs, resulting in small long-term trends (1960–2021).

Regarding anomalies, the change in the signs of anomalies for different decades is evident (Fig. 8). Positive anomalies (i.e., more dry days per year) appear in 1960-1969 and 2010–2019, as in those periods, extended droughts occurred, while wetter than average winters occurred during 1980–1989. Moreover, the period 1960–1969 displays positive anomalies, while in 1970–1979, the anomalies are smaller, followed by a positive anomaly during 1980–1989. So, we observe a decreasing trend -less dry days- in the period 1960–1989. Then, we observe more dry days from 1990 to 2019, but it is worth recalling the extended and persistent drought since 2010.

Nevertheless, statistical significance is limited to north of 35°S for 1960–1969 (more dry days) and 1980–1989 (less dry days). However, at higher thresholds (5 and 10 mm per

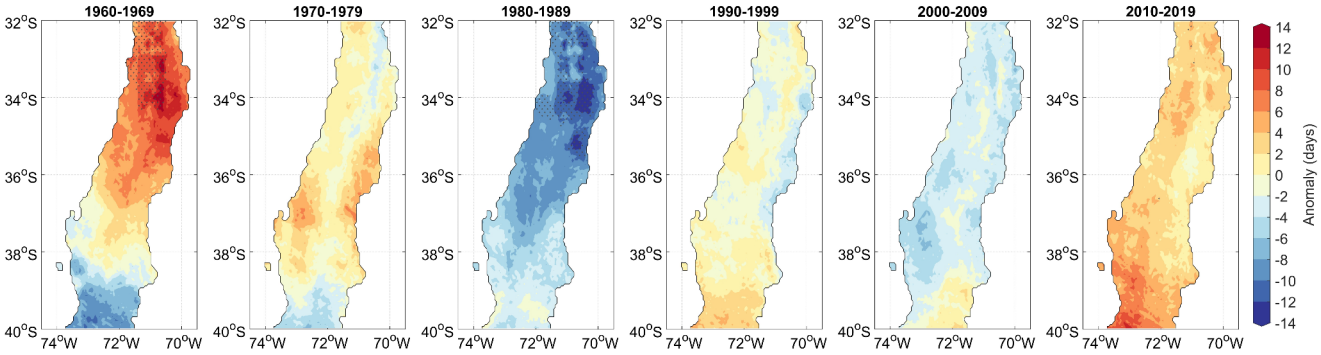

Fig. 8 Average decadal anomalies of annual dry days using the 1 mm threshold for defining dry days. Stippled areas indicate statistical significance at the 95% confidence level

day to define a dry day), the extent of the significant changes from 2010 to 2019 exhibits large areas of positive and significant anomalies, especially south of 34°S. Rain leading to fewer dry days is a trivial result. Still, the decadal variability highlights the importance of the number of dry days, the number of wet days, and annual amounts in planning. On a monthly scale, positive anomalies might have predominated during June 1960–1969, but July was the opposite in the same decade. Therefore, anomalies of different months are not necessarily representative of the anomalies developing during an entire season or year.

Regarding the statistical significance of anomalies, we also find considerable differences in the different months, which vary depending on the chosen threshold. Notably, in the last decade, from 2010 to 2019, positive anomalies are mostly present from April to July (especially in June), with each month having different areas of statistical significance. However, in all cases, this area expands as the threshold increases.

3.4 Climate Fields and dry days

The relationship between anomalies and trends in the number of dry days and composites of mean sea level pressure (MSLP), zonal wind on 500 hPa (u500), and sea surface temperature (SST) over the South Pacific is shown in Fig. 9. We centered our analysis between April and July since the average decadal anomalies of accumulated dry days between these months exhibited higher magnitudes and statistical significance than in the rest. Regarding wind anomalies, we focused our analysis on the zonal component since it is more important for precipitation and dry days anomalies in central Chile, given its predominance in mid-latitudes. Besides, we only show results for the 500 hPa level since anomaly patterns at the three analyzed levels are similar, although magnitudes differ. On the other hand, for simplicity's sake, we do not show results for geopotential height at 500 hPa; they are also closely correlated to SLP and u500 anomalies.

The relationship between dry day anomalies and MSLP is unclear (second row in Fig. 9). It is worth noting that clear patterns may not be apparent due to the somewhat arbitrary composite period composites, as they might mix different climate processes. However, as noted in Fig. 8, there are noticeable shifts in anomalies in dry days during the periods. However, positive anomalies of dry days tend to be associated with positive anomalies of MSLP on subtropical latitudes of the central eastern South Pacific, where the South Pacific Anticyclone is usually located. MSLP anomalies on higher latitudes are not always associated with dry days anomalies of a specific sign, notwithstanding that during the last decade. However, there have been large and significant negative MSLP anomalies on the Amundsen-Bellingausen Seas and significant positive anomalies of dry days in central Chile. Wind anomalies show a very interesting wavelike pattern that is clearer for some decades than others, particularly during 2010–2019, when magnitudes are highest. In general, when there are positive zonal wind anomalies in subtropical latitudes of eastern South Pacific and western South America and negative anomalies in mid-latitudes, negative anomalies of dry days are dominant in central Chile (and the opposite is also observed). On the other hand, SST anomalies do not show patterns that allow making clear associations with anomalies of dry days. Nevertheless, over the last two decades, especially the last one, positive and significant SST anomalies have been established on subtropical latitudes of the western South Pacific, concomitant to positive anomalies of dry days.

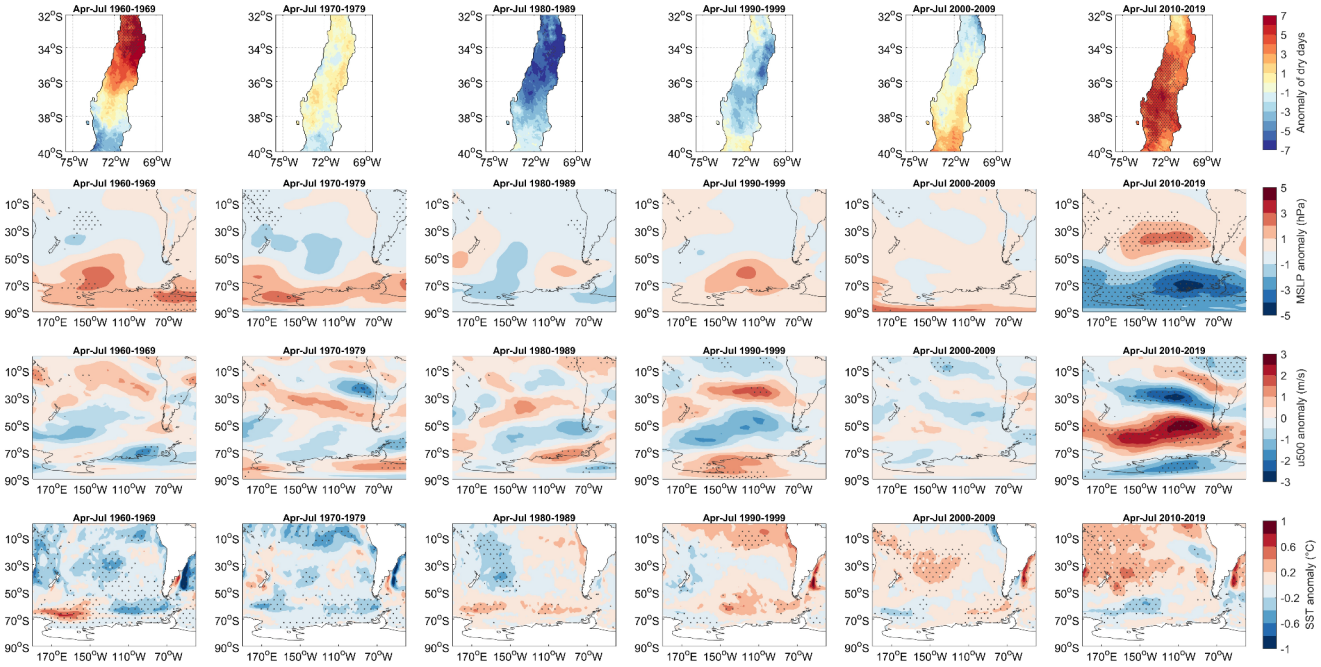

Fig. 9 Average decadal anomalies during June of dry days in central Chile (1 mm threshold), mean sea level pressure (MSLP), zonal wind at 500 hPa (u500), and sea surface temperature (SST) on the South Pacific area between the years 1960–2019. Stippled areas indicate statistically significant anomalies at 95% confidence level

4 Discussion

4.1 Trend's Sensitivity to Thresholding

In a global-scale study, Wainwright et al. (2022) indicates that dry-day trends and patterns may be sensitive to the threshold, especially in large spatial domains that include several climate types. Our study focused on an area with a homogenous climate where most agricultural activities occur, so a single threshold for all pixels is supported. Also, the five thresholds showed similar results (Fig. 7). However, further analysis includes the interdependence between dry and wet days at different thresholds.

4.2 Observed Anomalies in Climate Fields

Like most Mediterranean climates, Central Chile has experienced drier conditions over recent years (Seager et al. 2019), and dryness is expected to increase in the future (Polade et al. 2017). Precipitation deficits from 25–45%, the so-called "megadrought" (MD) as for its spatial and temporal extension (Boisier et al. 2016; Garreaud et al. 2017b, 2020), have had detrimental impacts on local hydrology, vegetation, and socioeconomic conditions (Garreaud et al. 2017b; González et al. 2018; Muñoz et al. 2020; Fuentealba et al. 2021; McCarthy et al. 2022). The exceptional length of the MD could have resulted from the prevalence of a circulation dipole characterized by deep tropospheric anticyclonic anomalies over the subtropical Pacific and cyclonic anomalies over the Amundsen-Bellingshausen Sea, hindering the passage of extratropical storms over central Chile (Garreaud et al. 2020). In this sense, more dry days during drought years would be related to a decrease in the number of weather systems crossing subtropical latitudes of South America (Garreaud et al. 2017a). However, the attribution of positive trends in dry days is to be cleared. From the meteorological perspective, at least half of the precipitation deficit during the mega-drought is related to natural forcing associated with decadal atmospheric and oceanic variability over the Pacific, and around a quarter by anthropogenic forcing (Boisier et al. 2016).

Large-scale modes of variability, such as El Niño-Southern Oscillation (ENSO), Southern Annular Mode (SAM), and Pacific Decadal Oscillation, are the most significant sources of interannual variability of precipitation in Central Chile (Boisier et al. 2018b; Aceituno et al. 2021; Montecinos and Aceituno 2003; Valdés-Pineda et al. 2016; Dogar et al. 2017a) and other regions (Dogar et al. 2017a). Warm ENSO phases are related to wetter conditions, while positive SAM is related to negative rainfall anomalies (Garreaud 2009). ENSO is the dominant mode, although its different configurations lead to different effects on precipitation amounts (Arias et al. 2021). For non-ENSO conditions, the complex interplay of sources of variability dumpers precipitation's predictability (Montecinos et al. 2011). During La Niña-events, the stormtrack moves poleward while

higher pressures in the subtropical Pacific and weaker mid-level westerlies. ENSO impacts in precipitation are weaker in summer than in winter (Dogar et al. 2017a, 2019; Dogar and Almazroui 2022). The combination of processes leads to precipitation deficits. The persistence of a dipole subtropical Pacific and cyclonic anomalies over the Amundsen Bellingshausen Sea has lowered the number of extratropical storms over central Chile since 2010, leading to more dry days (Garreaud et al. 2017a). Additionally, interannual variability through El Niño Southern Oscillation (ENSO) is a significant modulator of the aforementioned cyclonic-anticyclonic dipole of anomalies in the South Pacific (Garreaud et al. 2020), therefore affecting the number of annual dry days at such time scales.

Some studies have related the deepening of the Amundsen Sea Low (Fogt et al. 2012; Hosking et al. 2013; Turner et al. 2013), i. e. cyclonic/negative SLP anomalies over the Amundsen-Bellingnhausen Seas, to ozone depletion and changes in the strength and position of Southern Hemisphere's westerlies (England et al. 2016; O'Connor et al. 2021; Fogt and Zbacnik 2014). In contrast, others have suggested that Pacific sea surface temperature or other external forcing might be important drivers of its variability (Garreaud et al. 2021; Hosking et al. 2016). Following England et al. (2016), this deepening has been mainly observed during the summer months. However, our analysis shows it is also present during autumn and early winter (especially in June), along with positive SLP anomalies north of the Amundsen Low. Other authors have shown this result too, such as Garreaud et al. (2021), who also have related the existence of this SLP anomaly dipole to positive SST trends on western South Pacific over subtropical and mid-latitudes, which have been called "The Southern Blob" (SB). Moreover, the authors propose a dynamic mechanism that would explain the relationship and protagonism of the SB on the decline in precipitation in central Chile over the past decade. They also mention that other forcings, such as the Southern Annular Mode (SAM; Marshall 2003), could play a role in the observed variability.

The positive SST anomalies observed during the last decades in the West Pacific have been related to oceanic and atmospheric dynamics. Notably, it has been detected that the South Pacific Ocean Gyre has intensified and shifted poleward (Roemmich et al. 2007; Hitt et al. 2022), as other subtropical gyres also have (Yang et al. 2020), which would contribute to an increase of tropical and warm water transport to subtropical and mid-latitudes by the East Australian Current (Cai et al. 2005; Wu et al. 2012; Qu et al. 2019; Hitt et al. 2022; Li et al. 2022). This poleward shift would be influenced to a large degree by changes in the Southern Hemisphere's mid-latitude westerlies, particularly given their strengthening and poleward shift as well, which would also favor SAM's positive phase (Hall and Visbeck 2002; Zilberman et al. 2014; Hitt et al. 2022). Therefore, the western South Pacific SST anomalies suggested by Garreaud et al. (2009) as a relevant forcing of precipitation anomalies on central Chile over the last decade could be a consequence of changes in extratropical atmospheric circulation.

The annual mean SAM index has shown positive and significant trends throughout the 20th century, and when seasons are analyzed separately, austral summer shows the highest magnitude trends (Marshall 2003; Dätwyler et al. 2018; Fogt and Marshall 2020). However, there have been local and asymmetric variations on extratropical latitudes during other seasons that haven't been reflected on the zonally symmetric SAM, given its annular defined structure. For example, Schneider et al. (2015) shows that there have been important anomalies in the South Pacific area of magnitudes up to 3 times larger than the zonal average, and this area shows larger trends during autumn. These variations, albeit considerable in magnitude, usually are not considered part of the SAM, and therefore, neither are their effects. From this, the definition of the SAM may affect the results of any study employing it (Ho et al. 2012). In particular, the asymmetric variability of extratropical circulation in the Southern Hemisphere has been associated with a zonal wave three patterns (Franzke et al. 2015; Goyal et al. 2022) that is stronger in the Pacific Ocean (Renwick 2005; Campitelli et al. 2022), so it might be possible that these asymmetries have affected central Chile's precipitation. Furthermore, Campitelli et al. (2022) distinguished between the symmetric and asymmetric components of the SAM and found that both correlate with precipitation variations in central Chile. However, the symmetric component would have a more significant effect (especially on the central-southern area).

Seager et al. (2019), by using climate model simulations, indicates that the precipitation changes are associated with changes in moisture convergence and advection near and on the coast of subtropical South America, for which easterly wind anomalies would be necessary on the area. These anomalies and variations would result from the expansion of Hadley Cells and tropics, along with the poleward shift of mid-latitude westerlies and storm tracks, which would be related to anthropogenic forcing. In our results, we have also observed consistent wind anomalies with what is proposed by Seager et al. (2019); therefore, this mechanism could be at play. Nonetheless, a complete confirmation of these dynamical processes, and others reviewed in this section, would require further analysis since there are limitations on forming physical hypotheses based solely on using composites (Boschat et al. 2016).

Concerning the PCA analysis performed and its results, we found an inflection point for trends on the first PC in 1982, whose cause is still unrevealed. First, PCA/EOF

analysis results do not necessarily reflect a physical meaning (Dommenget and Latif 2002; Jolliffe 2003; Boschat et al. 2016). Still, given that this change in trends is also present in the time series of the defined clusters represented mainly by the first mode of variability, this change is likely not simply a product of a statistical rearrangement. In 1982, a very strong El Niño event occurred (Cane 1983) and implied pronounced positive accumulated precipitation anomalies in central Chile (Rutllant and Fuenzalida 1991), therefore negative anomalies of dry days (noticeable in Fig. 6 and verified pixels). This fact, in addition to the effect of the megadrought of the past decade, may have given rise to the differences in trends before and after 1982, despite the impact of the also very strong El Niño event of 1997 (Kane 1999; Cai et al. 2020). The verification of this hypothesis requires a closer examination.

The atmospheric-oceanic variability aspects that have been recognized as possible forcings of the previously mentioned variations, including central Chile's megadrought, are changes in the strength and position of Southern Hemisphere's westerlies, the Southern Annular Mode, expansion of the Hadley cell, South Pacific SST variability, among others. Since that drying has also been observed in other places with Mediterranean climate, both in the southern and northern hemispheres, and given that all of them have different forces influencing them, it is improbable to have occurred by a chance sampling of interannual variability (Seager et al. 2019). In the case of central Chile, each of the forcings above may contribute to the joint effect observed, even participating in positive or negative feedback processes. However, further research is needed to elucidate it.

4.3 Planning Implications

Longer dry periods and more extended regions affected by daily to weekly scales will impact how productive activities and cities adapt to a future warmer climate scenario. For instance, at seasonal time scales, understanding the patterns of time and space of wet/dry days provides a way to tailor water management practices. At larger temporal scales, this information becomes a valuable input for policy design and assessment, such as new water infrastructure or allocation of water rights (Barria et al. 2019). As the economic value of information increases with more extreme dry days frequency, modeling the extent and occurrence of dry days helps to assess future climate risks. As the leading cause for the MD is natural (Boisier et al. 2016), regardless of whether MD conditions remain or change, climate-based agricultural water management is crucial to ensure a sufficient productivity level and optimal water usage at seasonal scales, but also for planning at seasonal to inter-annual scales.

Moreover, Núñez et al. (2013, 2014), using Standardized Drought Indices, calls that proper use of drought indices must consider decadal climate variability. For instance, Sarricolea et al. (2019) shows that the annual and wet season Concentration Index showed positive and significant trends between 1970 and 1994 that were more evident than in any other period. This coincides with the warm (positive) phase of the PDO affecting Chile between 1976 and 1990 (Quintana and Aceituno 2012), representing a climatic shift in South America (Jacques Coper and Garreaud Salazar 2015). The trend change is observed in Figs. 6 and 8, and Table 1, where noticeable transitions from negative to positive anomalies have occurred for decades. This pattern underscores the decadal variability of the dry-days pattern. Even though the period selection is somewhat arbitrary, it is grounded on the observed changes.

A simultaneous decline in annual mean river flow has also been seen during megadrought (MD) years (2010–2019), which can be substantially more extensive than the rainfall deficit, leading to stronger water scarcity conditions. In this regard, coordination between irrigation procedures and dry days frequency becomes more essential to ensure the effectiveness of the former and deal with adverse conditions for agricultural development. For example, under MD conditions, some areas with natural vegetation over central Chile have decreased productivity during the growing season (September to January). In contrast, irrigated areas have been much less affected by reduced precipitation (Garreaud et al. 2017b; Zambrano-Bigiarini et al. 2017) due to investment in irrigation infrastructure to alleviate less rainfall. Yields of annual crops, such as wheat and maize, are expected to decrease in the range of 5–10%, and mainly small farmers perceive a significant decrease in productivity (Aldunce et al. 2017). Still, such changes could be mitigated by investing in more efficient irrigation systems (Meza et al. 2008, 2012). However, it must be stressed that as agriculture largely relies on rainfall, a drier climate makes the country more vulnerable to climate change (Boisier et al. 2018a; Peña-Guerrero et al. 2020).

Other forcings are volcanic eruption and anthropogenic activities. Even though there is a vast literature on short-term and medium-range effects of large volcanic eruptions (e.g., El Chichón in 1982 and Pinatubo in 1991) (cf. Dogar et al. 2017b; Dogar and Sato 2019; Dogar 2020; Paik et al. 2023) on circulation, there are few works on Chile. Volcanic aerosols can interact with atmospheric circulation patterns such as the Southern Annular Mode (SAM) and influence regional climate variability (Boisier et al. 2018b; Dogar et al. 2024). Moreover, changes in precipitation are predictable shortly after eruptions (Power et al. 2021). Regarding anthropogenic activities, the lasting and persistent drought since 2010 has had a noticeable impact on dry-day trends.

Also, circulation mechanisms and pattern changes have been extensively explored (Garreaud et al. 2017a, 2020, 2021). However, there is still a knowledge gap regarding the attribution of the observed trends in precipitation. Boisier et al. (2016) pioneered this endeavor, stating that one-quarter to one-third of the causes are attributable to anthropogenic activities. However, we stress that the effects of less precipitation are cascading to less available water (Boisier et al. 2018b) and are reinforced by increasing pressure over existing and scarce water resources (Boisier et al. 2024).

Our results indicate that the chosen study period may tremendously affect the final results and their interpretation. Particularly, observed atmospheric trends during 30–40 years and their analysis could lead to associating them to external forcings, when in reality, they could have been induced by low-frequency variability Grise et al. (2019). In our results, for example, the effect of the megadrought between 32–38°S cannot be observed on long-term trends (1960–2021), partly because the '60s were a decade particularly abundant on dry days, but when only the last 30 years are considered, the effect of the 2010–2020 dry decade on trends is evident. This fact does not necessarily mean that the megadrought is caused only by natural variability, but its attribution should be faced carefully. Concerning long-term significant trends, as seen in Fig. 7, they are mainly located south of 38°S, and given their robustness (they show up for all thresholds and time intervals analyzed), it is likely that they have been generated by external forcing. Nevertheless, natural variability can still play a role in these observed changes; thus, attributing these trends must be handled prudently.

5 Conclusions

The present study analyzed dry days in central Chile from 1960 to 2021 using gridded data products between 32 and 40 °S and five daily precipitation thresholds to define dry days. The pattern of accumulated dry days, both at monthly and annual scales, closely follows the corresponding accumulated precipitation pattern, showing a very similar latitudinal gradient and seasonal behavior. Shared variances indicate that precipitation frequency, represented by dry days, is generally a more important factor than intensity for modulating accumulated precipitation variations. Nevertheless, this relationship can vary in some places and occasions. Therefore, the interpretation of dry days results should always be cautious.

Temporal variability of dry days could be widely observed at inter-annual and longer time scales. In particular, linear trends over the entire study period show a long-term and significant increase in the annual number of dry days south of 38°S, while long-term trends north of this latitude are low in magnitude and nonsignificant. Moreover, the occurrence of central Chile's megadrought is detectable when average decadal anomalies between 2010 and 2019 are analyzed and when trends are calculated only in the second half of the study period, reflecting the high dependence of the trend's sign and magnitude on the analyzed time interval. This result could indicate an essential component of natural variability in generating the megadrought, although its great persistence and spatial extent also suggest that external forcing plays a substantial role.

These results directly affect water resources management in the context of increasing regional drought, providing key information for long-term planning, drought management, and adaptation to climate change. Spatial patterns tend to move southward, i.e., regions adapted to summer rainfall experience more dry days and less precipitation. Such variability and long-lasting droughts make trends sensitive to time frames, thus increasing uncertainty in planning and policy tasks.

Although this study has limitations, such as the exclusion of local factors and the uncertainties inherent to the dataset, use of linear trends, and climate systems forcing, it lays a solid foundation for future research to investigate the physical mechanisms underlying dry day variability and changes in trends.

In conclusion, this work highlights the role of dry days frequency in the hydroclimatic variability of central Chile and its strong modulation by internal climate variability on a decadal scale, a central aspect of the region's future sustainability. We comprehensively characterize the climatology and spatiotemporal variability of dry days from 1960 to 2021, identifying significant seasonal patterns and decadal trends, such as the increase of up to 10 days/decade in much of the region during the post1990 period. Frequency changes are influenced by the current drought that started in 2010. The variability of dry days showed significant links with large-scale climate patterns, such as the positive phase of the SAM and warm anomalies in the southwestern Pacific, suggesting a modulation by changes in the subtropical and extratropical atmospheric circulation.

The findings from this investigation into the temporal variability of dry days in Central Chile transcend mere statistical significance, providing pivotal insights with profound implications for regional and sectoral planning. These data illuminate the urgent need for robust, adaptive water resource management strategies to mitigate the impacts of increasingly prevalent and severe drought conditions. These climatic insights are valuable in agricultural domains, critically dependent upon predictable water availability. They enable the formulation of more resilient agricultural practices, including adopting drought-resistant crop varieties

and implementing advanced irrigation technologies. Furthermore, the delineation of dry-day trends offers essential guidance for policymakers. It underscores the necessity of transitioning from reactive drought responses to proactive, comprehensive climate change adaptation frameworks. This strategic pivot is crucial for enhancing water resources and agricultural systems' sustainability and resilience.

Acknowledgements We thank the financial support from FONDECYT 1230520, ANID/FONDAP/15130015, ANID/FONDAP/1523A0001 and ACT210080. The CR2MET data set is available at https://www.cr2.cl/datos-productos- grillados/. HadiSST v1.1 was retrieved from the National Center for Atmospheric Research at https://climatedataguide.ucar.edu/climate-data/sst-data-hadisst-v11.

Funding This research was funded by Agencia Nacional de Investigación y Desarollo grant FONDECYT 1230520. We also receive funding and support from ANID/FONDAP/15130015 and ANID/FONDAP/1523A0001.

Declarations

Conflict of interest On behalf of all authors, the corresponding author states that there is no conflict of interest.

References

Aceituno P, Boisier JP, Garreaud R et al (2021) Climate and weather in Chile. Water resources of Chile, pp 7–29

Aldunce P, Araya D, Sapiain R et al (2017) Local perception of drought impacts in a changing climate: the mega-drought in central Chile. Sustainability 9(11):2053

Anagnostopoulou C, Maheras P, Karacostas T et al (2003) Spatial and temporal analysis of dry spells in Greece. Theoret Appl Climatol 74:77–91

Apurv T, Sivapalan M, Cai X (2017) Understanding the role of climate characteristics in drought propagation. Water Resour Res 53(11):9304–9329

Arias PA, Garreaud R, Poveda G et al (2021) Hydroclimate of the andes part ii: hydroclimate variability and sub-continental patterns. Front Earth Sci 8:505467

Barrett BS, Hameed S (2017) Seasonal variability in precipitation in central and southern Chile: modulation by the South Pacific high. J Clim 30(1):55–69

Barria P, Rojas M, Moraga P et al (2019) Anthropocene and streamflow: Long-term perspective of streamflow variability and water rights. Elementa: Science of the Anthropocene 7(1)

Bartolini G, Betti G, Gozzini B et al (2022) Spatial and temporal changes in dry spells in a Mediterranean area: Tuscany (central Italy), 1955–2017. Int J Climatol 42(3):1670–1691

Boisier JP (2023) CR2MET: a high-resolution precipitation and temperature dataset for the period 1960–2021 in continental Chile. Zenodo. https://doi.org/10.5281/zenodo.7529682. https://doi.org/10.5281/zenodo.7529682

Boisier JP, Rondanelli R, Garreaud RD et al (2016) Anthropogenic and natural contributions to the Southeast Pacific precipitation decline and recent megadrought in central Chile. Geophys Res Lett 43(1):413–421

Boisier JP, Alvarez-Garret´on C, Cepeda J et al (2018a) CR2MET: A high-resolution precipitation and temperature dataset for hydroclimatic research in Chile. In: EGU General Assembly Conference Abstracts, p 19739

Boisier JP, Alvarez-Garreton C, Cordero RR et al (2018b) Anthropogenic drying in central-southern Chile evidenced by long-term observations and climate model simulations. Elementa: Science of the Anthropocene 6:74

Boisier JP, Alvarez-Garreton C, Marinao R et al (2024) Increasing water stress in Chile evidenced by novel datasets of water availability, land use and water use. EGUsphere 2024:1–50. https://doi.org/10.5194. https://egusphere.copernicus.org/preprints/2024/egusphere-2024-2695/ /egusphere-2024-2695, URL

Boschat G, Simmonds I, Purich A et al (2016) On the use of composite analyses to form physical hypotheses: an example from heat wave–SST associations. Sci Rep 6(1):29599

Burger F, Brock B, Montecinos A (2018) Seasonal and elevational contrasts in temperature trends in central Chile between 1979 and 2015. Glob Planet Change 162:136–147

Cai W, Shi G, Cowan T et al (2005) The response of the Southern Annular Mode, the East Australian Current, and the southern mid-latitude ocean circulation to global warming. Geophys Res Lett 32(23): L23706

Cai W, McPhaden MJ, Grimm AM et al (2020) Climate impacts of the El Niño– Southern Oscillation on South America. Nat Rev Earth Environ 1(4):215–231

Campitelli E, Díaz LB, Vera C (2022) Assessment of zonally symmetric and asymmetric components of the Southern Annular Mode using a novel approach. Clim Dyn 58(1–2):161–178

Cane MA (1983) Oceanographic events during El Nino. Science 222(4629):1189–1195

Catto J, Jakob C, Berry G et al (2012) Relating global precipitation to atmospheric fronts. Geophys Res Lett 39(10): L10805

Chen D, Dai A (2018) Dependence of estimated precipitation frequency and intensity on data resolution. Clim Dyn 50(9–10):3625–3647

Cindric K, Pasaric Z, Gajic-Capka M (2010) Spatial and temporal analysis of dry spells in Croatia. Theoret Appl Climatol 102:171–184

Dätwyler C, Neukom R, Abram NJ et al (2018) Teleconnection stationarity, variability and trends of the Southern Annular Mode (SAM) during the last millennium. Clim Dyn 51(5–6):2321–2339

Dogar MM (2020) Study of the regional climatic impacts of tropical explosive volcanism in the middle east and north africa region. PhD thesis, Hokkaido University

Dogar MMA, Almazroui M (2022) Revisiting the strong and weak enso teleconnec- tion impacts using a high-resolution atmospheric model. Atmos Environ 270:118866

Dogar MM, Sato T (2019) Regional climate response of middle eastern, African, and south Asian monsoon regions to explosive volcanism and enso forcing. J Geophys Research: Atmos 124(14):7580–7598

Dogar MM, Kucharski F, Azharuddin S (2017a) Study of the global and regional climatic impacts of enso magnitude using speedy agcm. J Earth Syst Sci 126(2):30
Dogar MM, Stenchikov G, Osipov S et al (2017b) Sensitivity of the regional climate in the Middle East and north africa to volcanic perturbations. J Geophys Research: Atmos 122(15):7922–7948
Dogar MM, Kucharski F, Sato T et al (2019) Towards understanding the global and regional climatic impacts of modoki magnitude. Glob Planet Change 172:223–241
Dogar MM, Fujiwara M, Zhao M et al (2024) Enso and Nao linkage to strong volcanism and associated post-volcanic high-latitude winter warming. Geophys Res Lett 51(1):e2023GL106114
Dommenget D, Latif M (2002) A cautionary note on the interpretation of EOFs. J Clim 15(2):216–225
England MR, Polvani LM, Smith KL et al (2016) Robust response of the Amundsen Sea Low to stratospheric ozone depletion. Geophys Res Lett 43(15):8207–8213
Fernández A, Muñoz A, González-Reyes A et al (2018) Dendrohydrology and´ water resources management in south-central Chile: lessons from the r´ıo imperial streamflow reconstruction. Hydrol Earth Syst Sci 22(5):2921–2935
Fogt RL, Marshall GJ (2020) The Southern Annular Mode: variability, trends, and climate impacts across the Southern Hemisphere. Wiley Interdisciplinary Reviews: Clim Change 11(4):e652
Fogt RL, Zbacnik EA (2014) Sensitivity of the Amundsen Sea low to stratospheric ozone depletion. J Clim 27(24):9383–9400
Fogt RL, Wovrosh AJ, Langen RA et al (2012) The characteristic variability and connection to the underlying synoptic activity of the Amundsen-Bellingshausen seas Low. J Geophys Rese Atmos 117: D07111
Franzke C, O'Kane T, Monselesan D et al (2015) Systematic attribution of observed Southern Hemisphere circulation trends to external forcing and internal variability. Nonlinear Process Geophys 22(5):513–525
Fuentealba M, Baham´ondez C, Sarricolea P et al (2021) The 2010–2020 megadrought drives reduction in lake surface area in the Andes of central Chile (32º-36ºs). J Hydrology: Reg Stud 38:100952
Garreaud RD (2009) The Andes climate and weather. Adv Geosci 22:3–11
Garreaud RD, Vuille M, Compagnucci R et al (2009) Present-Day South American climate. Palaeogeogr Palaeoclimatol Palaeoecol 281(3–4):180–195
Garreaud R, Falvey M, Montecinos A (2016) Orographic precipitation in coastal southern Chile: Mean distribution, temporal variability, and linear contribution. J Hydrometeorol 17(4):1185–1202
Garreaud R, Alvarez-Garreton C, Barichivich J et al (2017a) The 2010–2015 megadrought in central Chile: impacts on regional hydroclimate and vegetation. Hydrol Earth Syst Sci 21(12):6307–6327. https://doi.org/10.5194. https://www.hydrol-earth-syst-sci.net/21/6307/2017/ /hess-21-6307-2017, URL
Garreaud RD, Alvarez-Garreton C, Barichivich J et al (2017b) The 2010–2015 megadrought in central Chile: impacts on regional hydroclimate and vegetation. Hydrol Earth Syst Sci 21(12):6307–6327
Garreaud RD, Boisier JP, Rondanelli R et al (2020) The central Chile mega drought (2010–2018): a climate dynamics perspective. Int J Climatol 40(1):421–439
Garreaud RD, Clem K, Vicencio Veloso J (2021) The South Pacific pressure trend dipole and the Southern Blob. J Clim 34(18):7661–7676
Giorgi F, Raffaele F, Coppola E (2019) The response of precipitation characteristics to global warming from climate projections. Earth Sys Dyn 10(1):73–89
González ME, Gómez-González S, Lara A et al (2018) The 2010–2015 megadrought and its influence on the fire regime in central and south-central Chile. Ecosphere 9(8):e02300
Goyal R, Jucker M, Gupta AS et al (2022) A new zonal wave-3 index for the Southern Hemisphere. J Clim 35(15):5137–5149
Grise KM, Davis SM, Simpson IR et al (2019) Recent tropical expansion: natural variability or forced response? J Clim 32(5):1551–1571
Hall A, Visbeck M (2002) Synchronous variability in the Southern Hemisphere atmosphere, sea ice, and ocean resulting from the annular mode. J Clim 15(21):3043–3057
Hamed KH, Rao AR (1998) A modified Mann-Kendall trend test for autocorrelated data. J Hydrol 204(1–4):182–196
Hersbach H, Bell B, Berrisford P et al (2020) The ERA5 global reanalysis. Q J R Meteorol Soc 146(730):1999–2049
Hettiarachchi S, Wasko C, Sharma A (2022) Do longer dry spells associated with warmer years compound the stress on global water resources? Earth's Future 10(2): e2021EF002392
Hitt NT, Sinclair DJ, Neil HL et al (2022) Natural cycles in South Pacific gyre strength and the Southern Annular Mode. Sci Rep 12(1):18090
Ho M, Kiem A, Verdon-Kidd D (2012) The Southern Annular Mode: a comparison of indices. Hydrol Earth Syst Sci 16(3):967–982
Hosking JS, Orr A, Marshall GJ et al (2013) The influence of the Amundsen– Bellingshausen seas low on the climate of West Antarctica and its representation in coupled climate model simulations. J Clim 26(17):6633–6648
Hosking JS, Orr A, Bracegirdle TJ et al (2016) Future circulation changes off West Antarctica: sensitivity of the Amundsen Sea Low to projected anthropogenic forcing. Geophys Res Lett 43(1):367–376
Hoskins BJ, Hodges KI (2005) A new perspective on Southern Hemisphere storm tracks. J Clim 18(20):4108–4129
IPCC (2021) Climate Change 2021: The Physical Science Basis. Contribution of Working Group I to the Sixth Assessment Report of the Intergovernmental Panel on Climate Change, vol In Press. Cambridge University Press, Cambridge, United Kingdom and New York, NY, USA, https://doi.org/10.1017/9781009157896
Jacques Coper M, Garreaud Salazar R (2015) Characterization of the 1970s climate shift in South America. Int J Climatol 35:2164–2179
Jolliffe IT (2003) A cautionary note on artificial examples of EOFs. J Clim 16(7):1084–1086
Jolliffe I (2005) Principal component analysis. Encyclopedia of statistics in behavioral science
Kane R (1999) Some characteristics and precipitation effects of the El Nin˜o of 1997–1998. J Atmos Solar Terr Phys 61(18):1325–1346
Lagos-Zúñiga M, Mendoza PA, Campos D et al (2024) Trends in seasonal precipitation extremes and associated temperatures along continental Chile. Clim Dyn 64:4205–4222
Li J, Roughan M, Kerry C (2022) Drivers of ocean warming in the western boundary currents of the Southern Hemisphere. Nat Clim Change 12(10):901–909
Ma S, Zhou T, Dai A et al (2015) Observed changes in the distributions of daily precipitation frequency and amount over China from 1960 to 2013. J Clim 28(17):6960–6978
Marinovic I, Cindric Kalin K, Güttler I et al (2021) Dry spells in Croatia: observed climate change and climate projections. Atmosphere 12(5):652
Marshall GJ (2003) Trends in the Southern Annular Mode from observations and reanalyses. J Clim 16(24):4134–4143
Martínez-Retureta R, Aguayo M, Abreu NJ et al (2021) Estimation of the climate change impact on the hydrological balance in basins of south-central Chile. Water 13(6):794

McCarthy M, Meier F, Fatichi S et al (2022) Glacier contributions to river discharge during the current Chilean megadrought. Earth's Future 10(10):e2022EF002852

Meza FJ, Hansen JW, Osgood D (2008) Economic value of seasonal climate forecasts for agriculture: review of ex-ante assessments and recommendations for future research. J Appl Meteorol Climatology 47(5):1269–1286

Meza FJ, Wilks DS, Gurovich L et al (2012) Impacts of climate change on irrigated agriculture in the maipo basin, Chile: reliability of water rights and changes in the demand for irrigation. J Water Resour Plan Manag 138(5):421–430

Ministerio del Medio Ambiente C (2020) Informe del estado del medio ambiente

Montecinos A, Aceituno P (2003) Seasonality of the ENSO-related rainfall variability in central Chile and associated circulation anomalies. J Clim 16(2):281–296

Montecinos A, D´ıaz A, Aceituno P (2000) Seasonal diagnostic and predictability of rainfall in subtropical south America based on tropical pacific sst. J Clim 13(4):746–758

Montecinos A, Kurgansky MV, Mun˜oz C et al (2011) Non-enso interannual rainfall variability in central Chile during austral winter. Theoret Appl Climatol 106(3):557–568. https://doi.org/10. 1007/s00704-011-0457-1, URL

Motamedi A, Gohari A, Haghighi AT (2023) Three-decade assessment of dry and wet spells change across Iran, a fingerprint of climate change. Sci Rep 13(1):2888

Muñoz AA, Klock-Barría K, Alvarez-Garreton C et al (2020) Water crisis in Petorca Basin, Chile: the combined effects of a megadrought and water management. Water 12(3):648

Núñez J, Rivera D, Oyarzún R et al (2013) Influence of pacific ocean multidecadal variability on the distributional properties of hydrological variables in north-central Chile. J Hydrol 501:227–240

Núñez J, Rivera D, Oyarzún R et al (2014) On the use of standardized drought indices under decadal climate variability: critical assessment and drought policy implications. J Hydrol 517:458–470

O'Connor GK, Steig EJ, Hakim GJ et al (2021) Strengthening Southern Hemisphere Westerlies and Amundsen Sea low deepening over the 20th century revealed by proxy-data assimilation. Geophys Res Lett 48(24): e2021GL095999

Paik S, Min SK, Son SW et al (2023) Impact of volcanic eruptions on extratropical atmospheric circulations: review, revisit and future directions. Environ Res Lett 18(6):063003

Peña-Guerrero MD, Nauditt A, Muñoz-Robles C et al (2020) Drought impacts on water quality and potential implications for agricultural production in the maipo river basin, central Chile. Hydrol Sci J 65(6):1005–1021

Pica-Téllez A, Garreaud R, Meza R et al (2020) Informe proyecto arclim: Atlas de riesgos climáticos para chile. Centro de Ciencia del Clima y la Resiliencia, Centro de Cambio Global UC y meteodata para el Ministerio del Medio Ambiente a través de la Deutsche Gesellschaft für Internationale Zusammenarbeit (giz). Santiago, Chile

Pierce DW, Cayan DR, Das T et al (2013) The key role of heavy precipitation events in climate model disagreements of future annual precipitation changes in california. J Clim 26(16):5879–5896

Polade SD, Pierce DW, Cayan DR et al (2014a) The key role of dry days in changing regional climate and precipitation regimes. Sci Rep 4(1):4364

Polade SD, Pierce DW, Cayan DR et al (2014b) The key role of dry days in changing regional climate and precipitation regimes. Sci Rep 4:4364 EP –. URL. https://doi.org/10.1038/srep04364

Polade SD, Gershunov A, Cayan DR et al (2017) Precipitation in a warming world: assessing projected hydro-climate changes in California and other Mediterranean climate regions. Sci Rep 7(1):10783

Power S, Lengaigne M, Capotondi A et al (2021) Decadal climate variability in the tropical pacific: characteristics, causes, predictability, and prospects. Science 374(6563):eaay9165

Qu T, Fukumori I, Fine RA (2019) Spin-up of the southern hemisphere super gyre. J Geophys Research: Oceans 124(1):154–170

Quintana J, Aceituno P (2012) Changes in the rainfall regime along the extratropical west coast of south America (Chile): 30–43º s. Atmósfera 25(1):1–22

Ratan R, Venugopal V (2013) Wet and dry spell characteristics of global tropical rainfall. Water Resour Res 49(6):3830–3841

Rayner NA, Parker DE, Horton EB et al (2003) Global analyses of sea surface temperature, sea ice, and night marine air temperature since the late nineteenth century. J Phys Res 159(D14):4407. https://doi.org/10.1029/2002JD002670

Renwick JA (2005) Persistent positive anomalies in the Southern Hemisphere circulation. Mon Weather Rev 133(4):977–988

Rivera JA, Penalba OC, Betolli ML (2013) Inter-annual and interdecadal variability of dry days in Argentina. Int J Climatol 33(4):834–842

Roemmich D, Gilson J, Davis R et al (2007) Decadal spinup of the South Pacific subtropical gyre. J Phys Oceanogr 37(2):162–173

Rubio-Alvarez E, McPhee J (2010) Patterns of spatial and temporal variability in streamflow records in South Central Chile in the period 1952–2003. Water Resour Res 46(5): W05514

Rutllant J, Fuenzalida H (1991) Synoptic aspects of the central Chile rainfall variability associated with the Southern Oscillation. Int J Climatol 11(1):63–76

Sangüesa C, Pizarro R, Ibañez A et al (2018) Spatial and temporal analysis of rainfall concentration using the gini index and PCI. Water 10(2):112

Sarricolea P, Herrera-Ossandon M, Meseguer-Ruiz O (2017) Climatic regionalisation´ of continental Chile. J Maps 13(2):66–73

Sarricolea P, Meseguer-Ruiz O, Serrano-Notivoli R et al (2019) Trends of daily pre-´ cipitation concentration in central-southern Chile. Atmos Res 215:85–98

Schneider DP, Deser C, Fan T (2015) Comparing the impacts of tropical SST variability and polar stratospheric ozone loss on the Southern Ocean westerly winds. J Clim 28(23):9350–9372

Seager R, Osborn TJ, Kushnir Y et al (2019) Climate variability and change of Mediterranean-type climates. J Clim 32(10):2887–2915

Tabari H, Willems P (2018) More prolonged droughts by the end of the century in the Middle East. Environ Res Lett 13(10):104005

Turner J, Phillips T, Hosking JS et al (2013) The Amundsen Sea low. Int J Climatol 33(7):1818–1829

Valdés-Pineda R, Valdes JB, Diaz HF et al (2016) Analysis of spatio-temporal changes in annual and seasonal precipitation variability in south america-chile and related ocean–atmosphere circulation patterns. Int J Climatol 36(8):2979–3001

Valdés-Pineda R, Cañon J, Valdés JB (2018) Multi-decadal 40-to 60-year cycles of precipitation variability in Chile (south America) and their relationship to the amo and pdo signals. J Hydrol 556:1153–1170

Van Loon A, Laaha G (2015) Hydrological drought severity explained by climate and catchment characteristics. J Hydrol 526:3–14

Viale M, Garreaud R (2015) Orographic effects of the subtropical and extratropical Andes on upwind precipitating clouds. J Geophys Research: Atmos 120(10):4962–4974

Wainwright CM, Allan RP, Black E (2022) Consistent trends in dry spell length in recent observations and future projections. Geophys Res Lett 49(12):e2021GL097231

Wang X, Lu H, Yuan W (2022) Inter-annual variations of precipitation modulate the dry spell length. GeoHealth 6(4):e2022GH000611

Wetterhall F, Winsemius H, Dutra E et al (2015) Seasonal predictions of agrometeorological drought indicators for the limpopo basin. Hydrol Earth Syst Sci 19(6):2577–2586

Wilks DS (2005) Statistical methods in the atmospheric sciences. International geophysics. Elsevier Science, Amsterdam

Wilks DS (2011) Statistical methods in the atmospheric sciences. Academic press

Wu L, Cai W, Zhang L et al (2012) Enhanced warming over the global subtropical western boundary currents. Nat Clim Change 2(3):161–166

Yang H, Lohmann G, Krebs-Kanzow U et al (2020) Poleward shift of the major ocean gyres detected in a warming climate. Geophys Res Lett 47(5):e2019GL085868

Zambrano F, Wardlow B, Tadesse T et al (2017) Evaluating satellite-derived longterm historical precipitation datasets for drought monitoring in Chile. Atmos Res 186:26–42. https://doi.org/10.1016/j.atmosres.2016.11.006. http://www.sciencedirect.com/science/article/pii/S0169809516305865

Zambrano-Bigiarini M, Nauditt A, Birkel C et al (2017) Temporal and spatial evaluation of satellite-based rainfall estimates across the complex topographical and climatic gradients of Chile. Hydrol Earth Syst Sci 21(2):1295–1320

Zilberman N, Roemmich D, Gille S (2014) Meridional volume transport in the South Pacific: Mean and SAM-related variability. J Geophys Research: Oceans 119(4):2658–2678

Zolina O, Simmer C, Belyaev K et al (2013) Changes in the duration of European wet and dry spells during the last 60 years. J Clim 26(6):2022–2047